AIAA SciTech Forum
6-10 January 2025, Orlando, FL
AIAA SCITECH 2025 Forum

10.2514/6.2025-2502

CMAS Infiltration Studies on Thermal Barrier Coatings under Thermal Gradients Using Synchrotron X-Ray Diffraction

Zachary Stein*, Jan Erik Förster†
Embry-Riddle Aeronautical University, Daytona Beach, FL, 32114, USA

Peter Kenesei‡, Jun-Sang Park‡, Jonathan Almer‡
Advanced Photon Source, Argonne National Laboratory, Lemont, IL 60439, USA

Janine Wischek§, Marion Bartsch§, Uwe Schulz§, Ravisankar Naraparaju§
German Aerospace Center, 51147 Cologne, Germany

Seetha Raghavan¶
Embry-Riddle Aeronautical University, Daytona Beach, FL 32114, USA

High temperature ceramic protective coatings, also called thermal barrier coatings (TBCs), are used to protect components, which are internally or back-side cooled. Calcium-magnesium-alumino-silicate (CMAS) particulates, such as sand, are ingested by these aero-engines and travel through the hot gas stream, eventually depositing onto the TBCs. The subsequent degradation is detrimental to the lifetime of the coatings with the risk of engine failure. In this work, synchrotron X-ray diffraction measurements were used to capture effects CMAS has on a 7-8 wt% yttria-stabilized zirconia (YSZ) TBC applied on an internally cooled hollow dogbone sample under thermal gradient conditions. Thermochemical degradation of the YSZ coating was observed, after 1 hour of CMAS-infiltration, through the formation of monoclinic phase. The monoclinic phase concentration was observed to be around 18% at the surface of the YSZ coating and declining towards zero halfway through the coating. This monoclinic concentration is roughly 2 times less than under isothermal conditions at similar annealing temperatures and timescales. These results showcase the successful capture and monitoring of coating degradation throughout a replicated aircraft flight cycle. These results can be further expanded upon with other coating systems, to elucidate the transitory processes of in-situ coating degradation throughout an operational cycle. The results may be used in strategies to mitigate the detrimental effects of CMAS on high temperature ceramics.

*Graduate Student, Aerospace Engineering, Embry-Riddle Aeronautical University, Daytona Beach, FL, 32114, USA
†Post Doctoral Fellow, Aerospace Engineering, Embry-Riddle Aeronautical University, Daytona Beach, FL, 32114, USA
‡Beamline Scientist, Advanced Photon Source, Argonne National Laboratory, Lemont, IL 60439, USA
§Material Research Scientist, Institute of Materials Research, German Aerospace Center, 51147 Cologne, Germany
¶Professor, Aerospace Engineering, Embry-Riddle Aeronautical University, Daytona Beach, FL 32114, USA, AIAA Associate Fellow, raghavs3@erau.edu

I. Nomenclature

$7YSZ$	=	7 wt% (8 mol%) yttria stabilized zirconia
$CMAS$	=	Calcium-magnesium-alumino-silicate
$mPVF$	=	Monoclinic phase volume fraction
TBC	=	Thermal barrier coating
XRD	=	X-ray diffraction

II. Introduction

Superalloy components used within gas turbine engines for aerospace applications are susceptible to the high temperatures and harsh environments present during engine operation. High temperature ceramic coatings, known as thermal barrier coatings (TBCs), are applied through various deposition methods in order to insulate and protect these superalloy components [1]. Coupled with cooling methods, higher engine efficiencies are viable due to the increase in capacity for engine operating temperatures. A standard TBC used on turbine blades is comprised around 150 - 200 µm thick ceramic top coat layer of 7-8 wt% yttria-stabilized zirconia (7YSZ) and experiences a typical temperature difference of about 150 - 200°C from the hot gas stream surface of the coating to its interface [1–4]. Yttria is used as a stabilizer to the zirconia, stabilizing the polymorph into its metastable tetragonal phase at room temperature and prohibiting increased strain in the coating due to the roughly 4% volume expansion associated with the martensitic transformation [5, 6]. This work captured the degradation mechanism of a standard 7YSZ TBC using high energy synchrotron x-rays.

Electron-beam physical vapor deposition (EB-PVD) is standard deposition method used to apply TBCs onto high strained components, such as turbine blades, within the engine [1]. A higher in-plane strain tolerance can be achieved through EB-PVD due to its columnar microstructure that forms during the deposition process. The microstructure itself can be further tailored by modifying the deposition parameters, as reported previously in literature [7, 8].

During an aircraft's operation, particulates, such as calcium-magnesium-aluminosilicates (CMAS), are inevitably ingested by the engine. CMAS compositions, such as sand, then travel with the gas stream and become molten in the combustor. These molten sand particulates then flow to the turbine section of the engine and deposit onto the surface of the hot ceramic coating of the turbine blade. This CMAS melt, upon contact, begins to wet, infiltrate, and interact with the ceramic, causing irreparable coating degradation. This degradation can be categorized by thermochemical and thermomechanical mechanisms as the CMAS attack destabilizes the coating and introduces additional stresses into the coating itself [9, 10]. Capillary effects from the columnar microstructure of EB-PVD TBCs accelerate the infiltration of CMAS, essentially drawing the CMAS into the intercolumnar gaps present through the ceramic's microstructure [8]. Fig 1a summarizes the CMAS infiltration and its effects on the ceramic coating. Fig. 1b and Fig. 1c show SEM micrographs of pristine, non-infiltrated 7YSZ EB-PVD coating and CMAS-infiltrated counterpart 7YSZ EB-PVD coating, respectively. Some thermochemically induced phase destabilization of the ceramic coating is indicated through the monoclinic phase, denoted in Fig. 1c as mYSZ.

This CMAS-related degradation limits the operational capabilities of aircrafts operating in regions with high CMAS concentration by reducing the durability and lifetime of the essential high temperature ceramic coatings within the aircraft's engines. Capturing, monitoring, and elucidating the complex CMAS infiltration phenomenon and the subsequent CMAS-TBC interactions during operation is indispensable towards improving CMAS mitigation strategies.

Previous studies have looked at using in-situ synchrotron XRD to study the behaviors representative of operating conditions and its effects as a result of rapidly changing environments for ceramic coatings throughout a flight cycle [11–16]. This work builds upon these studies by capturing the effects of CMAS infiltration over the course of a 1-hour operation flight cycle with thermal gradient conditions. Synchrotron x-rays offer high spatial and temporal resolution capabilities, which is necessary to capture the fast acting effects CMAS has on high temperature ceramic coatings.

III. Experimental Methods

A. High Temperature Ceramic Coatings Sample Manufacturing

A 7-8 wt% yttria-stabilized zirconia (YSZ) ceramic coated tubular IN100 specimen was used in this study. The roughly 211±4 µmm YSZ ceramic coating was deposited on top of a 118±4 µmm NiCoCrAlY bond coat which was applied on the IN100 substrate through electron beam physical vapor deposition. A similar tubular dogbone sample and

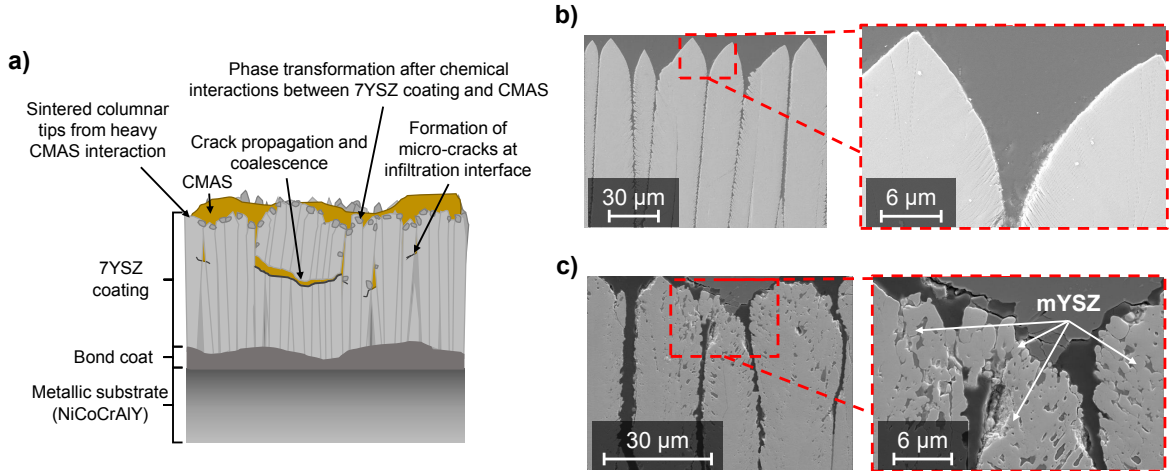

Fig. 1 a) Schematic of CMAS infiltration and its effects on 7YSZ coatings, [10], b) SEM micrograph of a pristine, non-infiltrated 7YSZ coating, and c) SEM micrograph of a CMAS infiltrated 7YSZ coating with progressed thermochemical degradation and sintering.

experimental setup was used in previous work by Knipe et al. [11]. Fig. 2a shows a schematic of the experimental setup. An x-ray incident beam impinged the surface of the coated sample in a grazing manner and produced a diffraction cone of Debye-Scherrer rings unique to the crystalline phase of the material present in the beam path. These diffraction rings are captured by an area detector during experiments. Fig. 2b focuses on a fourth of the Debye-Scherrer rings of stabilized tetragonal 7YSZ; the 7YSZ diffraction peaks are identified and denoted using Miller indices. An examplary x-ray diffraction lineout generated from area detector images is depicted in Fig. 2c. The temperature profile used during this infiltration experiment is shown in Fig. 2d.

It should be noted that the sample was thermally cycled for about 130 hours prior to this study. Each pre-aging cycle lasted roughly 80 minutes and includes a 20 minute ramp up to operation temperatures, 40 minute hold, and finally a 20 minute ramp down to room temperature. The tubular dogbone sample had inner and outer radii of 2 and 4 mm, respectively, which allowed for a thermal gradient to be established through internal cooling of the inner wall of the substrate and outer heating of the surface of the ceramic coating.

B. CMAS Fabrication & Composition

The CMAS used in this work this study was synthesized from compositions found within aero-engines operating in the Middle East (in mol.%: 24.6% CaO, 12.4% MgO, 11% Al_2O_3, 41.7% SiO_2, 8.7% FeO & 1.6% TiO_2); this composition has been characterized and used in previous studies [8–10]. The CMAS powders were artificially synthesized through the co-decomposition of SiO_2, TiO_2, and Me-nitrates powders. This processing of the CMAS powders is described in greater detail in previous work [8].

C. CMAS Infiltration Parameters & Thermal Gradient Cycle Profile

A paste of the CMAS powder, with a concentration of roughly 10 mg/cm^2, was applied in vertical strips on the ceramic surface of the tubular dogbone sample. The infiltration experiments conducted within this study were performed with annealing temperatures of 1260 °C and with heating and cooling rates of 300 °C/min within an IR Heater consisting of four 2000 W lamps with elliptical mirrors to focus the energy onto the sample. Measurements were performed at room temperature after the end of the 1 hour of CMAS infiltration, as shown in Fig. 2d.

Thermal gradient was established through pressurized air flowing through the internal cooling channel of the hollow, tubular dogbone sample. Previous work had shown an air flow of 75 SLPM results in a 150 °C temperature difference between the coating surface and bond coat [11]. Therefore under similar experimental conditions and sample geometry, a similar thermal gradient resulting in a temperature difference of approximately 150 °C across the thickness of the coating can be established. Within this work, an air flow rate of 80 SLPM was used and held throughout the entire thermal cycle. This slight increase in flow rate was to achieve a similar thermal gradient while operating at higher

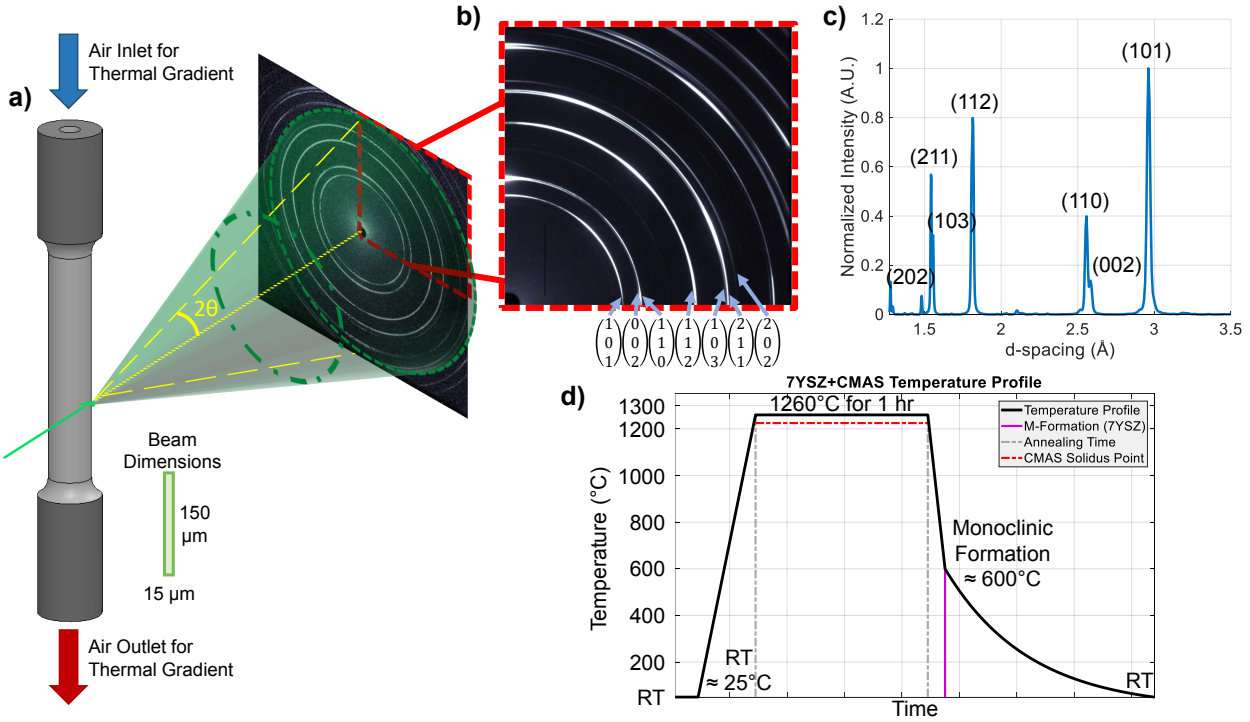

Fig. 2 a) Schematic of the hollow cylindrical dogbone sample highlighting the incident X-ray beam penetrating the coating in a grazing manner and the resulting diffraction cone of Debye-Scherrer rings, b) zoom of a fourth of the Debye-Scherrer rings for 7YSZ with the Miller indices of the intensity peaks identified and labeled, c) the 1D XRD lineout of the Debye-Scherrer rings with the same main peaks identified and labeled, and d) the temperature profile of the experiment, highlighting the 1 hr of CMAS infiltration at 1260 °C and the formation of the monoclinic phase of the ceramic coating around 600 °C as a result of phase destabilization from CMAS-related thermochemical degradation.

surface temperatures during testing.

D. In-situ synchrotron XRD Experimental Parameters

High-energy XRD measurements were performed at the 1-ID beamline of the Advanced Photon Source at Argonne National Laboratory. The tubular dogbone sample was mounted inside of the IR furnace with K-type thermocouples placed on the surface of the sample as well as at the inlet and outlets of the internal cooling channel of the heated test section. The furnace and sample were moved relative to the beam through a micrometer stage to graze further into the coating during measurements. The incident beam size was 15 μm horizontally by 150 μm vertically with an beam energy of 90.515 keV. This beam size provides roughly 14 data points across the ceramic layer. The incident beam impinged the sample and diffracted. Full Debye-Scherrer diffraction rings were captured on a GE-41RT 2048 x 2048 pixel area detector with a sample to detector distance of roughly 1800 mm. CeO_2 powder was used to calibrate the instrument. The infiltration experimental data was collected with an exposure time of 0.3 s. A maximum depth of 225 μm relative to the surface of the sample was probed to fully capture the ceramic topcoat of the sample. Due to the curvature of the tubular dogbone sample, the probed volume varied from 0.00138 mm^3 near the surface to 0.00806 mm^3 at the maximum measured depth. The changing probed volume effects as a result of grazing have been considered through the changing transmission measurements captured for each data point. High-energy XRD using a synchrotron was selected due to the high spatial resolution, fast data acquisition, and penetration depth, all of which are vital for understanding the transitory mechanisms and processes initiated as CMAS infiltrates and degrades the ceramic coating.

E. Monoclinic Phase Volume Fraction (mPVF) Equation

$$mPVF(\%) = \frac{I_m(\bar{1}11) + I_m(111)}{I_t(101) + I_m(\bar{1}11) + I_m(111)} \tag{1}$$

An equation for the phase volume fraction for YSZ coatings, with respect to the martensitic, monoclinic phase, has been previously reported in literature and is presented in Eq. 1 [17]. Variables for Eq. 1 are obtained through the integrated intensities of the monoclinic $(\bar{1}11)$, (111) and tetragonal (101) XRD peaks. Pseudo-Voigt fittings were used in the deconvolution of the XRD peaks to isolate the respective monoclinic and tetragonal peaks of interest.

IV. Results & Discussion

A cutout section of the dogbone sample is shown in Fig. 3a. This cutout clearly depicts the internal air cooling channel as well as a proportionally accurate representation of the thermal barrier coating layer of the sample. Fig. 3b depicts a detail of this cutout, focusing on the ceramic layer. The CMAS-related thermochemical degradation, quantified through the monoclinic phase formation is tracked and plotted in contour maps throughout the depth of the 7YSZ layer within Fig. 3b.

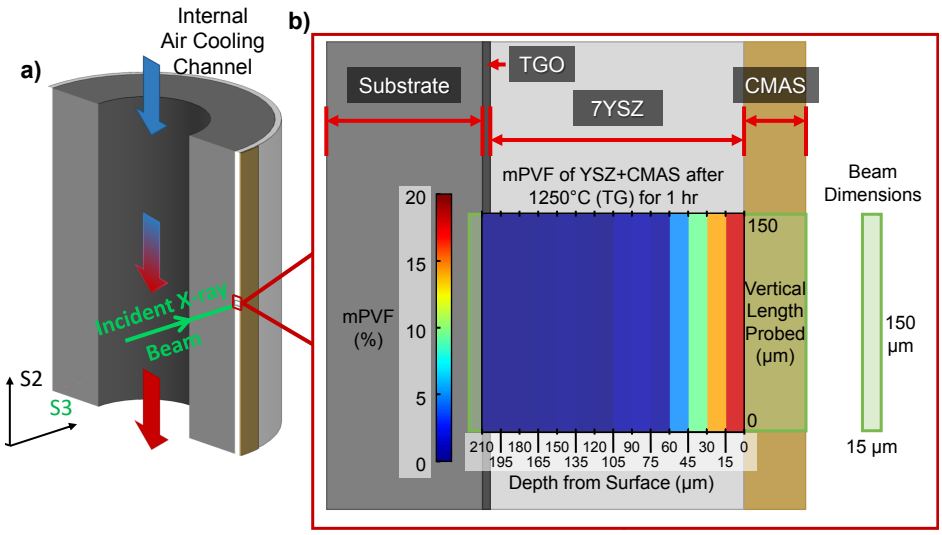

Fig. 3 a) Proportional schematic cutout of the cylindrical dogbone sample and b) a detail of the cutout exposed to CMAS along with the spatial resolution of the incident X-ray beam measured throughout the depth of the coating. A contour map highlights the monoclinic phase volume fraction throughout the depth of the ceramic 7YSZ coating layer.

From the contour map in Fig. 3b, it can be observed the highest monoclinic phase volume fraction concentrations within the 7YSZ coating occurs at the surface of the coating, closest to the CMAS deposition and CMAS-7YSZ interfacing region. A gradient of the monoclinic concentration then occurs until reaching essentially zero after 105 μm. This trend is a result of the longer time of exposure interactions, higher concentrations of CMAS near the surface of the coating, and greater surface area coverage of the 7YSZ for the CMAS to interact with. The thermal gradient through the depth of the ceramic layer also greatly impacts the mechanisms influencing CMAS degradation within the coating. Due to the presence of a thermal gradient, there exists a point through the thickness of the 7YSZ ceramic coating layer where the temperature would be below the CMAS melting temperature and therefore any CMAS infiltrating to this point solidified. Once solidified, the CMAS has a greatly reduced interaction with the ceramic coating.

The thermal gradient effects can be observed within the plot in Fig. 4, which displays the monoclinic PVF after thermal exposure under thermal gradient and isothermal conditions, respectively. The sample for the isothermal experiment had a CMAS paste deposited onto the surface of a 12 by 12 mm square with an approximately 400 μm thick 7YSZ coating that was EB-PVD deposited onto an alumina substrate. This sample was then annealed at 1250 °C for

1-hour in a furnace. Synchrotron x-ray diffraction measurements were then conducted after CMAS infiltration at room temperature.

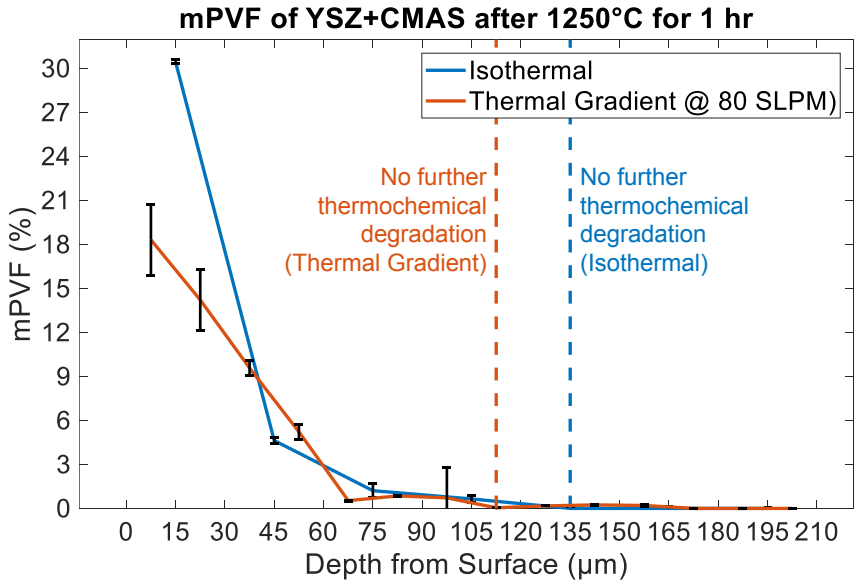

Fig. 4 The monoclinic phase volume fraction of 7YSZ ceramic coatings exposed to CMAS for 1 hr around 1250 °C under isothermal (blue) and thermal gradient (orange) temperature profile conditions. The thermal gradient infiltration condition was performed with air flowing over the backside of the underlying substrate of the sample at 80 standard liters per minute.

It should be noted that the spatial resolutions of the data in the previously published work, [15], presenting the monoclinic PVF after isothermal exposure and after thermal gradient condition presented within this study are different. The incident beam size within the isothermal condition was 30 μm by 300 μm while the beam size within the thermal gradient condition was 15 μm by 150 μm, horizontal by vertical, respectively. Therefore, the isothermal line within Fig. 4 was plotted with a 15 μm offset to place the mPVF values within the middle of probed region; similarly, the thermal gradient line was plotted with a 7.5 μm offset. These offsets were applied to aid in the comparison of the different spatially resolved data.

Using Eq. 1, it can be observed within Fig. 4 the isothermal condition experienced around 2 times the amount of mPVF concentration present near the surface of the coating as compared to the thermal gradient condition. Then after approximately 45 μm from the surface of the coating, the two thermal loading conditions appear to follow similar values throughout the depth of the two coatings. In the experiment under isothermal conditions, it was observed that CMAS was fully infiltrated within a few minutes of exposure at 1250 °C. Given the similar thermal gradient conditions as reported in [11], a 150 °C temperature difference can be assumed within the thermal gradient sample. This thermal gradient is assumed to have hindered full CMAS infiltration. Future work by the authors plan to directly observe the depth of CMAS infiltration. Discrepancies with the isothermal condition between full CMAS infiltration and the formation of monoclinic phase, indicating thermochemical degradation, is likely due to phase destabilization of the coating occurring much slower than the physical CMAS infiltration [8]. In other words, there is a lag between CMAS infiltration and subsequent phase change. It is expected, similar to the results of previously published work within the isothermal case reported in [15], further exposing the thermal gradient sample to 10 hours of infiltration would show an increase in the mPVF concentrations within the CMAS infiltrated regions; however, more future work is needed to test this expectation. From Fig. 4, it is noted that the monoclinic YSZ phase was not observed beyond the depth of 135 μm for the isothermal case as compared to 112.5 μm for the thermal gradient case. This observation highlights the more severe condition (isothermal) has a more detrimental effect on the TBC than the thermal gradient case, overstating the extent of thermochemical degradation influencing coating failure. Optimization of the thermal gradient profile to extend the life of the TBC and minimizing the effects of CMAS infiltration can be attained using XRD data. The current data suggests a thermal gradient across the depth of the coating of approximately 150 °C results in roughly halving the effect of phase destabilization and reducing the thermochemical degradation of the coating near the surface and columnar tips

of the 7YSZ EB-PVD coatings.

V. Conclusion

High temperature ceramic coatings are used to protect superalloys within the aircraft gas turbine engine during operation. These coatings are exposed to extreme environments. Exposure to debris and particulates, such as sand, is inevitable when operating within sandy regions such as deserts. Exposure to this sand, degrades these ceramic coatings, risking pre-mature coating failure and potentially catastrophic engine failure during operation. Replicating the environmental conditions and capturing the transitory interactions from first contact exposure and throughout a operational cycle during flight in a controlled manner is vital to better elucidate and mitigate the detrimental pre-mature coating failure mechanisms. This work has demonstrated a way to non-destructively capturing CMAS infiltration through synchrotron X-ray diffraction methods. Thermochemical degradation of the coating was observed through the formation of the monoclinic phase through the 7-8 wt% yttria-stabilized zirconia ceramic coating after 1 hour of infiltration. Additional data can be captured to monitor the interactions of the CMAS with the ceramic coating throughout the thermal cycle to better unveil the stages and processes of degradation due to CMAS-coating interactions at high temperatures simulating operational flight conditions within a gas turbine engine.

Acknowledgments

This research used resources of the Advanced Photon Source, a U.S. Department of Energy (DOE) Office of Science User Facility operated for the DOE Office of Science by Argonne National Laboratory under Contract No. DE-AC02-06CH11357. Funding: This material is based upon work supported by National Science Foundation grant OISE 1952523, Fulbright Academic Grant, the Department of Defense (DoD) through the National Defense Science & Engineering Graduate (NDSEG) Fellowship Program, and the German Science Foundation (DFG) in the frame of the collaborative project SFB TRR 103.

References

[1] Thakare, J. G., Pandey, C., Mahapatra, M., and Mulik, R. S., "Thermal barrier coatings—A state of the art review," *Metals and Materials International*, Vol. 27, 2021, pp. 1947–1968.

[2] Miller, R. A., "Thermal barrier coatings for aircraft engines: history and directions," *Journal of thermal spray technology*, Vol. 6, No. 1, 1997, pp. 35–42.

[3] Knipe, K., Manero II, A., Siddiqui, S. F., Meid, C., Wischek, J., Okasinski, J., Almer, J., Karlsson, A. M., Bartsch, M., and Raghavan, S., "Inside the Engine Environment–Synchrotrons Reveal Secrets of High-Temperature Ceramic Coatings," *American Ceramic Society Bulletin*, Vol. 94, No. 1, 2015, p. 22.

[4] Sobhanverdi, R., and Akbari, A., "Porosity and microstructural features of plasma sprayed Yttria stabilized Zirconia thermal barrier coatings," *Ceramics International*, Vol. 41, No. 10, 2015, pp. 14517–14528.

[5] Chen, L., "Yttria-stabilized zirconia thermal barrier coatings—a review," *Surface Review and Letters*, Vol. 13, No. 05, 2006, pp. 535–544.

[6] Viazzi, C., Deboni, A., Ferreira, J. Z., Bonino, J.-P., and Ansart, F., "Synthesis of Yttria Stabilized Zirconia by sol–gel route: Influence of experimental parameters and large scale production," *Solid State Sciences*, Vol. 8, No. 9, 2006, pp. 1023–1028.

[7] Schulz, U., Saruhan, B., Fritscher, K., and Leyens, C., "Review on advanced EB-PVD ceramic topcoats for TBC applications," *International journal of applied ceramic technology*, Vol. 1, No. 4, 2004, pp. 302–315.

[8] Naraparaju, R., Hüttermann, M., Schulz, U., and Mechnich, P., "Tailoring the EB-PVD columnar microstructure to mitigate the infiltration of CMAS in 7YSZ thermal barrier coatings," *Journal of the European Ceramic Society*, Vol. 37, No. 1, 2017, pp. 261–270.

[9] Barrett, C., Stein, Z., Hernandez, J., Naraparaju, R., Schulz, U., Tetard, L., and Raghavan, S., "Detrimental effects of sand ingression in jet engine ceramic coatings captured with Raman-based 3D rendering," *J. Eur. Ceram. Soc.*, Vol. 41, No. 2, 2021, pp. 1664–1671.

[10] Stein, Z., Naraparaju, R., Schulz, U., Tetard, L., and Raghavan, S., "Residual stress effects of CMAS infiltration in high temperature jet engine ceramic coatings captured non-destructively with confocal Raman-based 3D rendering," *Journal of the European Ceramic Society*, 2022.

[11] Knipe, K., Manero, A., Siddiqui, S. F., Meid, C., Wischek, J., Okasinski, J., Almer, J., Karlsson, A. M., Bartsch, M., and Raghavan, S., "Strain response of thermal barrier coatings captured under extreme engine environments through synchrotron X-ray diffraction," *Nature communications*, Vol. 5, No. 1, 2014, pp. 1–7.

[12] Diaz, R., Mossaddad, M., Bozan, A., Raghavan, S., Almer, J., Okasinski, J., Palaez-Perez, H., and Imbrie, P., "In-situ strain measurements of EB-PVD thermal barrier coatings using synchrotron x-ray diffraction under thermo-mechanical loading," *49th AIAA Aerospace Sciences Meeting including the New Horizons Forum and Aerospace Exposition*, 2011, p. 500.

[13] Manero, A., Sofronsky, S., Knipe, K., Meid, C., Wischek, J., Okasinski, J., Almer, J., Karlsson, A. M., Raghavan, S., and Bartsch, M., "Monitoring local strain in a thermal barrier coating system under thermal mechanical gas turbine operating conditions," *JOM*, Vol. 67, No. 7, 2015, pp. 1528–1539.

[14] Manero, A., Knipe, K., Wischek, J., Meid, C., Okasinski, J., Almer, J., Karlsson, A. M., Bartsch, M., and Raghavan, S., "Capturing the competing influence of thermal and mechanical loads on the strain of turbine blade coatings via high energy X-rays," *Coatings*, Vol. 8, No. 9, 2018, p. 320.

[15] Stein, Z., Kenesei, P., Park, J.-S., Almer, J., Naraparaju, R., Schulz, U., and Raghavan, S., "High-energy X-ray phase analysis of CMAS-infiltrated 7YSZ thermal barrier coatings: Effect of time and temperature," *Journal of Materials Research*, 2020, pp. 1–11.

[16] Fouliard, Q., Hernandez, J., Heeg, B., Ghosh, R., and Raghavan, S., "Phosphor thermometry instrumentation for synchronized acquisition of luminescence lifetime decay and intensity on thermal barrier coatings," *Measurement Science and Technology*, Vol. 31, No. 5, 2020, p. 054007.

[17] Garvie, R. C., and Nicholson, P. S., "Structure and thermomechanical properties of partially stabilized zirconia in the CaO-ZrO2 system," *Journal of the American Ceramic Society*, Vol. 55, No. 3, 1972, pp. 152–157.